

doi:10.3969/j.issn.1672-4623.2020.09.014

# 基于 Sentinel-1A 数据的南京市水体信息提取

陈媛媛<sup>1</sup>, 郑加柱<sup>1</sup>, 魏浩翰<sup>1</sup>, 张荣春<sup>2</sup>, 房星旭<sup>1</sup>

(1. 南京林业大学, 江苏 南京 210037; 2. 南京邮电大学, 江苏 南京 210023)



**摘要:** 基于先进的 Sentinel-1A SAR 数据, 对南京地区的水体覆盖信息进行提取, 首先对 SAR 图像进行滤波、辐射校正以及几何校正等预处理; 再利用灰度共生矩阵提取影像中的纹理信息, 并结合散射强度信息, 利用 SVM 算法进行初分类; 然后利用地形信息提取山体; 最后从初分类结果中剔除山体阴影, 得到水体提取结果。通过对比实验发现, 该方法可有效去除山体阴影以及淹水期水田的影响, 减少对水体信息的混淆, 使结果与真实地表更加接近。研究结果能为南京市的水资源管理部门提供相应的理论支撑。

**关键词:** SAR; 水体信息提取; 纹理特征; DEM; SVM

**中图分类号:** P237

**文献标志码:** B

**文章编号:** 1672-4623(2020)09-0062-04

城市水资源分布情况与城镇居民的生产生活息息相关, 因此精准提取城市水资源分布信息将对水资源调查和水利规划产生积极的影响。南京市水域面积达 11% 以上, 采用先进技术对南京市水体进行监测和信息提取具有重要意义。目前城市水资源调查的常规手段包括光学遥感数据和人工调查<sup>[1-3]</sup>, 人工调查费时费力, 光学遥感受光照、水汽、天气状况影响较大, 因此上述手段均受到一定的限制。合成孔径雷达 (SAR) 作为工作在微波波段的新遥感技术, 穿透力强, 具有全天时全天候的工作能力。近年来, 随着越来越多的 SAR 传感器 (Envisat、ALOS PALSAR、RadarSat-2、TerraSAR、Sentinel-1A/B、高分三号等) 相继发射升空以及 SAR 数据逐步产品化, SAR 图像在资源调查中的应用潜力逐渐被发掘出来<sup>[4-5]</sup>。利用 SAR 影像提取城市水体信息的研究很多, 但如何提高提取精度、减少阴影的影响仍是一个被热烈讨论的问题<sup>[6-7]</sup>。本文基于先进的 Sentinel-1A SAR 数据, 对南京地区的水体覆盖信息进行了提取。

## 1 理论基础

### 1.1 基于灰度共生矩阵的纹理特征提取

灰度共生矩阵是一种基于统计分析的纹理特征提取方法, 也是通过研究图像灰度的空间相关特性来描述纹理的常用方法之一。1973 年, 该方法由 Haralick 提出, 统计了两个像素点位置的联合概率分布, 提供了图像的灰度方向、间隔以及变化幅度的信息, 但不能直接提供纹理特征, 只能通过间接的计算从灰度共生矩阵中提取作为纹理分析的一些特征参量<sup>[8-9]</sup>。

Haralick 提出了 14 种特征参量, 本文采用熵 (en)、均匀性 (hom)、角二阶矩 (ASM) 和差异性 (dis) 4 种, 计算公式为:

$$en = - \sum_{i=0}^{Ng-1} \sum_{j=0}^{Ng-1} g(i, j) \log(g(i, j)) \quad (1)$$

$$hom = \sum_{i=0}^{Ng-1} \sum_{j=0}^{Ng-1} \frac{g(i, j)}{1 + |i - j|} \quad (2)$$

$$ASM = \sum_{i=0}^{Ng-1} \sum_{j=0}^{Ng-1} g(i, j)^2 \quad (3)$$

$$dis = \sum_{i=0}^{Ng-1} \sum_{j=0}^{Ng-1} |i - j| g(i, j) \quad (4)$$

式中,  $P(i, j)$  为灰度共生矩阵中像素对出现的次数;

$Ng$  为图像量化后的灰度级别;  $g(i, j) = \frac{P(i, j)}{\sum_{i=0}^{Ng-1} \sum_{j=0}^{Ng-1} P(i, j)}$ ,

可理解为对灰度共生矩阵进行归一化处理。

### 1.2 SVM 算法

SVM 算法是一种常见的基于机器学习的分类方法, 被广泛应用于遥感图像的地物分类中<sup>[10-12]</sup>。该算法基于结构风险最小化原理, 先在特征空间构建一个最优超平面, 再求解全局最优解, 即在整个样本空间的期望拟合某个概率上界, 在满足分类的限制条件下, 尽可能地把分类数据集中的所有点分开, 且使点与该超平面距离最远。最优超平面的计算公式为:

$$f(x) = \omega \times x + b = 0 \quad (5)$$

式中,  $x_i (i=1, \dots, N)$  为训练样本输入;  $y_i \in \{+1, -1\}$  为期望输出;  $\omega$  为权值矢量;  $b$  为阈值。所要寻找的最优分类超平面能将不同的类分开, 同时使分类间隔达到最大。

**收稿日期:** 2019-01-02。

**项目来源:** 江苏省测绘地理信息科研资助项目 (JSCHKY201708); 江苏省自然科学基金资助项目 (BK20180779); 南京林业大学青年科技创新基金资助项目 (CX2018015)。

SVM 算法的主要原理可简单概括为：对于线性可分的情况，进行分析分类；对于不能进行线性划分的情况，利用若干非线性的映射算法把低维输入空间的线性不可分的样本转化到高维特征空间内，使其变得线性可分。

## 2 实验分析

### 2.1 实验数据与预处理

本文采用的数据为 2016 年 5 月获取的覆盖南京市的 Sentinel-1A 数据。Sentinel-1A 遥感卫星于 2014 年 4 月 3 日在法属圭亚那发射升空入轨，是欧空局“哥白尼计划”发射的第一颗环境监测卫星，搭载 C 波段 SAR 系统，轨道高度为 693 km，重访周期为 12 d。该传感器具有宽幅模式（IW）、波模式（WV）、条带模式（SM）和超宽幅模式（EW）4 种成像模式，本文采用 IW 模式图像进行南京市水体信息的提取。该模式下获取的 SAR 影像分辨率为  $5\text{ m} \times 20\text{ m}$ ，幅宽为 240 km。实验所用影像覆盖了南京市主城区和其他部分地区，但六合和高淳的部分区域未被覆盖。南京市的水体主要包括流经本市的长江、秦淮河、玄武湖等。

对数据进行水体提取前，为了增加图像的可读性需进行多视处理、滤波、辐射校正、几何校正等一系列预处理。由于下载的原始数据是三视的，为了不降低图像的空间分辨率，本文没有再对图像进行多视处理，只进行了滤波处理。本文分别采用 Frost 滤波器、基于边缘保护的滤波器和 LEE 滤波器在  $3 \times 3$  窗口大

小下对图像进行滤波，并对滤波效果进行目视解译和比较（图 1）。结果表明，采用 Frost 滤波器滤波后的图像上仍有很多斑点噪声，而采用基于边缘保护的滤波器滤波后的图像中地物边缘变得模糊，因此通过对比，本文决定选用 LEE 滤波器。通过比较 LEE 滤波器在不同窗口尺寸下的滤波效果发现（图 2）， $3 \times 3$  窗口下依然存在很多斑点噪声；而窗口尺寸大于  $5 \times 5$  时，图像的细节损失严重，一些地物的纹理信息变得模糊，因此本文采用  $5 \times 5$  窗口的 LEE 滤波器对图像进行滤波。对滤波后的图像进行辐射校正和几何校正处理；再利用灰度共生矩阵提取图像中的纹理特征；然后结合纹理特征与散射强度信息，利用 SVM 算法提取图像中的水体；最后选用 90 m 的 SRTM DEM 文件生成山体斜率，对斜率数据进行处理提取图像中的山体，并从上一过程结果中剔除山体阴影的影响，得到最终的水体提取结果。纹理特征图像的局部放大图如图 3 所示，矩形和椭圆形中地物分别为农田和水体，发现二者的纹理特征有显著差异。具体水体提取流程如图 4 所示。

### 2.2 实验结果与分析

本文还利用主成分分析法（PCA）、最近邻算法（KNN）以及无纹理和 DEM 信息的 SVM 算法对图像进行水体信息的提取，并与本文方法进行对比，结果如图 5 所示。由于监督分类中样本的选择对最后结果有一定的影响，因此实验采用同一组训练样本进行精度计算，结果如表 1 所示。

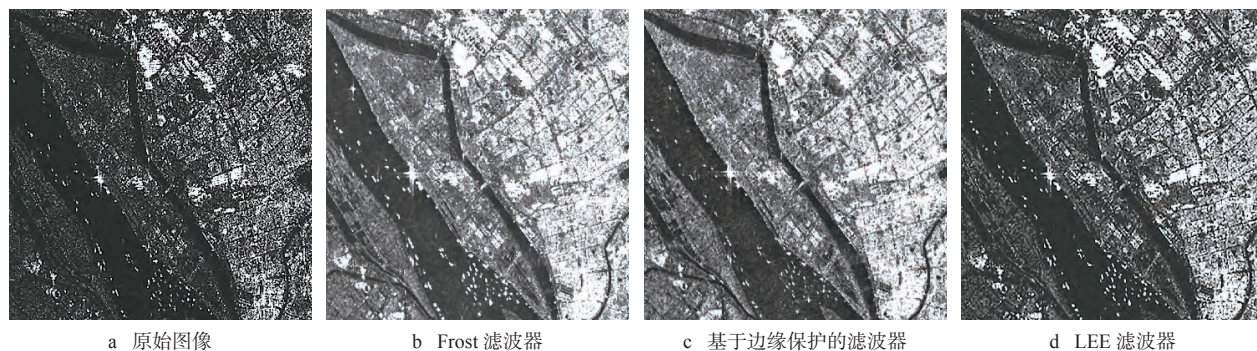


图 1 不同滤波器在  $3 \times 3$  窗口下的滤波效果

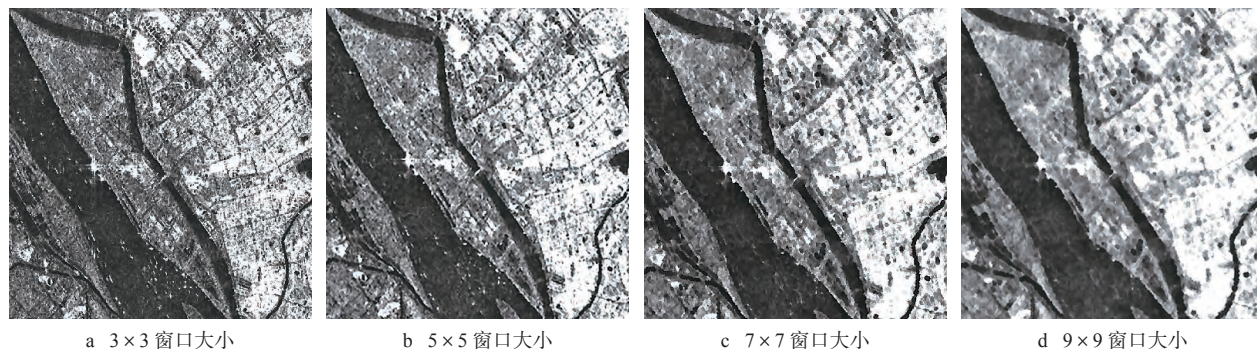


图 2 LEE 滤波器在不同窗口下的滤波效果



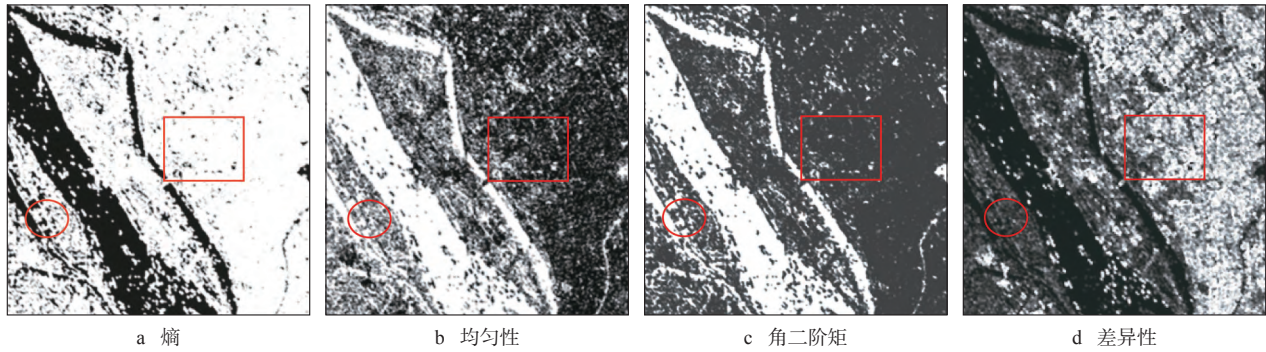


图 3 纹理特征局部放大图

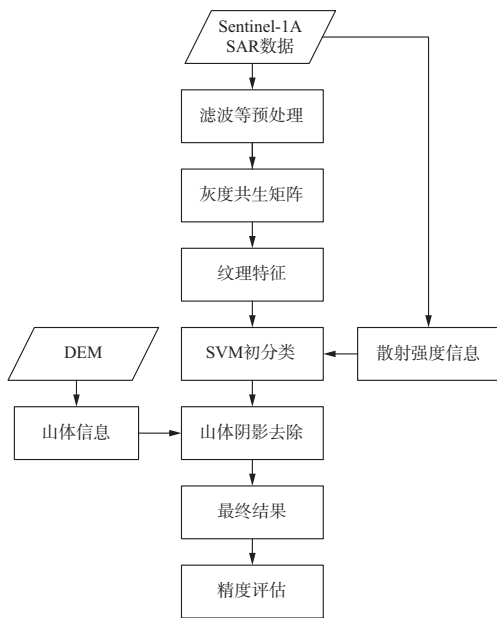


图 4 水体信息提取流程图

由图 5 可知, PCA 法和 KNN 法的提取结果均不如 SVM 算法, 前两种算法对于水体提取的用户精度均在 63% 以下, 生产者精度也不足 85%, 分类结果中很多零碎地物被误分为水体, 这种情况在 SVM 算法的提取结果 (图 5c) 中得到了很大改善。然而, 通过与南京地区的高分辨率光学影像和 Google Earth 比

较发现, 图 5c 中有部分农田被错分为水体 (如椭圆区域), 其原因在于影像获取期间这些地区的水田刚好处于淹水期, 水田里的水与城市中水体均发生奇次散射, 在 SAR 图像上呈现相同的散射特征; 而三角形区域的山体阴影和矩形框中的禄口机场也被误分为水体, 前者是因为山体阴面接收不到 SAR 信号, 导致在 SAR 图像上呈现暗色调; 后者是因为机场大面积的水泥跑道也发生奇次散射, 呈现与水体相似的散射特性。加入纹理信息和 DEM 后 (图 5d), 上述情况得到了极大改善, 这是因为农田排列整齐, 农田中分布的田埂使其呈现与水体明显不同的纹理特征 (图 3); 机场的熵与水体的熵也有很大不同, 所以当加入熵这个纹理特征后, 也能把机场剔除; 山体都有一定的斜率, 加入地形信息后, 由山体阴影产生的误分也可被消除。

由表 1 可知, 利用本文方法提取水体的用户精度和生产者精度分别为 97.90% 和 98.32%, 总体精度和 Kappa 系数达到了 98.90% 和 0.974 1, 比 PCA 法和 KNN 法提高了 35% 以上, 比无纹理和 DEM 信息的 SVM 算法, 总体精度提高了 15% 以上。由此可见, 本文方法在提取 Sentinel-1A 图像中的水体方面具有一定的优越性。

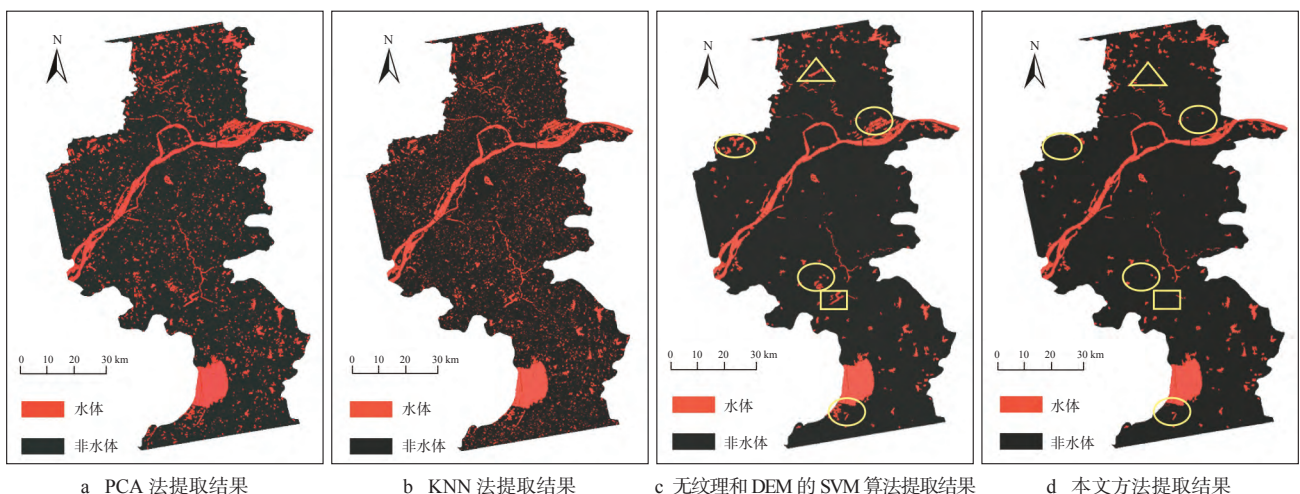


图 5 不同方法提取结果比较

表 1 分类精度

提取方法		用户精度 /%	生产者 精度/%	总体精度 /%	Kappa 系数
PCA 法	水体	62.54	84.62	85.40	0.693 6
	非水体	95.15	85.62		
KNN 法	水体	60.54	84.98	85.00	0.685 5
	非水体	95.44	85.01		
无纹理和 DEM 的 SVM 算法	水体	81.27	91.01	92.00	0.823 3
	非水体	96.58	92.36		
本文方法	水体	97.90	98.32	98.90	0.974 1
	非水体	99.29	99.15		

### 3 结 语

本文利用 C 波段 Sentinel-1A SAR 数据对南京市进行了水体信息提取, 通过对比实验可得到以下结论: 在水体提取方面, SVM 算法比 PCA 法和 KNN 法具有更好的适用性; 纹理特征可有效减少机场以及淹水期水田与城市水体的混淆; 地形信息可去除山体阴影对水体提取的影响; 本文方法得到的结果与真实地表更加接近, 总体精度和 Kappa 系数分别达到 98.90% 和 0.974 1。实验验证了 Sentinel-1A 数据在城市水体提取中的有效性, 能为相关部门管理城市水资源提供相应的参考。

### 参考文献

[1] 都金康, 黄永胜, 冯学智, 等. SPOT 卫星影像的水体提取方法

及分类研究[J]. 遥感学报, 2001, 5(3): 214-219

- [2] 杜云艳, 周成虎. 水体的遥感信息自动提取方法[J]. 遥感学报, 1998, 2(4): 364-369
- [3] 睦海刚, 陈光, 胡传文, 等. 光学遥感影像与 GIS 数据一体化的水体分割、配准与提取方法[J]. 武汉大学学报(信息科学版), 2016, 41(9): 1 145-1 150
- [4] CHEN Y Y, HE X F, WANG J. Classification of Coastal Wetlands in Eastern China Using Polarimetric SAR Data[J]. Arabian Journal of Geosciences, 2015, 8(12): 10 203-10 211
- [5] 叶子伟, 陈小松, 吴敦. 基于 Radarsat SAR 微波影像的水体提取研究[J]. 测绘地理信息, 2016, 41(2): 54-57
- [6] 庞科臣, 陈立福, 王思雨. 融合 DEM 去除山体阴影的水体提取方法[J]. 电子科技, 2016, 29(4): 76-78
- [7] 杨存建, 魏一鸣, 王思远, 等. 基于 DEM 的 SAR 图像洪水水体的提取[J]. 自然灾害学报, 2002, 11(3): 121-125
- [8] Haralick R M, Shanmugam K, Dinstein I. Textural Features for Image Classification[J]. IEEE Transactions on Systems, Man and Cybernetics, 1973, 3(6): 610-621
- [9] 安智晖, 余洁, 刘利敏. 结合纹理信息的极化 SAR 影像分类研究[J]. 地理空间信息, 2016, 14(2): 41-43
- [10] 陈媛媛, 何秀凤, 王静. 基于 SVM 的极化 SAR 沿海滩涂分类[J]. 地理空间信息, 2015, 13(6): 150-153
- [11] 骆剑承, 周成虎, 梁怡, 等. 支撑向量机及其遥感影像空间特征提取和分类的应用研究[J]. 遥感学报, 2002, 6(1): 50-55
- [12] 冉琼, 于浩洋, 高连如, 等. 结合超像元和子空间投影支持向量机的高光谱图像分类[J]. 中国图象图形学报, 2018, 23(1): 95-105

**第一作者简介:** 陈媛媛, 博士, 讲师, 主要从事微波遥感信息提取方面的研究。

### (上接第 61 页)

- [13] 宫清华, 黄光庆, 郭敏, 等. 基于 GIS 技术的广东省洪涝灾害风险区划[J]. 自然灾害学报, 2009, 18(1): 58-63
- [14] 张若琳, 孟晖, 连建发. 基于 GIS 的中国泥石流易发性评价[J]. 成都理工大学学报(自然科学版), 2013, 40(4): 379-386
- [15] 陈述彭, 鲁学军, 周成虎. 地理信息系统导论[M]. 北京: 科学出版社, 1999
- [16] 席盼盼. 基于 GIS 的朗县地质灾害易发性评价研究[D]. 长春: 吉林大学, 2014
- [17] 邱海军. 区域滑坡崩塌地质灾害特征分析及其易发性和危险性评价研究: 以宁强县为例[D]. 西安: 西北大学, 2012
- [18] 王哲, 易发成. 基于层次分析法的绵阳市地质灾害易发性评价[J]. 自然灾害学报, 2009, 18(1): 14-23
- [19] 陈圣劼, 尹东屏, 李玉涛, 等. 南京地区城郊降雨差异特征分析[J]. 气象与环境学报, 2016, 32(6): 27-33
- [20] 张建云, 王银堂, 贺瑞敏, 等. 中国城市洪涝问题及成因分析[J]. 水科学进展, 2016, 27(4): 485-491
- [21] 丁一汇, 张建云. 暴雨洪涝[M]. 北京: 气象出版社, 2009
- [22] 魏凤英. 现代气候统计诊断与预测技术[M]. 第 2 版. 北京: 气象出版社, 2007: 43-44, 63-66
- [23] 中国气象局. 高温科普五: 什么是高温热浪?[EB/OL]. (2011-10-26) [2018-12-13]. [http://www.cma.gov.cn/2011qx/fw/2011qxkx/2011qkpd/201110/t20111026\\_124192.html](http://www.cma.gov.cn/2011qx/fw/2011qxkx/2011qkpd/201110/t20111026_124192.html)
- [24] Atkinson B W. The Reality of the Urban Effect on Precipitation,

a Case Study Approach[J]. Urban Climate, 1979, 108: 342-360

- [25] Parry M. An "Urban Rainstorm" in the Reading Area[J]. Weather, 1956, 11: 41-48
- [26] Harnack R P, Landsberg H E. Selected Case of Convective Precipitation Caused by the Metropolitan Area of Washington, D.C.[J]. Journal of Applied Meteorology, 1975, 14: 1 050-1 060
- [27] 朱秀迪, 张强, 孙鹏. 北京市快速城市化对短时间尺度降水时空特征影响及成因[J]. 地理学报, 2018, 73(11): 56-60
- [28] 陈艺文. 城市绿地的海绵效应研究[D]. 南京: 东南大学, 2017
- [29] 邢大伟, 张玉芳, 粟晓玲. 陕西关中城市防灾抗灾能力评估[J]. 西北水工程与水工程, 1997(3): 10-14
- [30] 饶恩明, 肖毅, 欧阳志云. 中国湖库洪水调蓄功能评价[J]. 自然资源学报, 2014, 29(8): 1 356-1 365
- [31] 章文波, 符素华, 刘宝元. 目估法测量植被覆盖度的精度分析[J]. 北京师范大学学报(自然科学版), 2001, 37(3): 402-408
- [32] 李苗苗. 植被覆盖度的遥感估算方法研究[D]. 北京: 中国科学院研究生院(遥感应用研究所), 2003
- [33] 刘洋洋, 李永强, 李有鹏. AHP-模糊综合评价法在山区丘陵公路边坡危险性评估中的应用[J]. 河南科学, 2018, 36(2): 237-244
- [34] 张建云, 王银堂, 刘翠善, 等. 中国城市洪涝及防治标准讨论[J]. 水力发电学报, 2017, 36(1): 1-6

**第一作者简介:** 刘娜, 硕士, 工程师, 主要从事气候变化对水文水资源影响的研究工作。



### Research on the Spatial Distribution Variation of the Populus Euphratica in the Mainstream of Tarim River

by GU Fang

**Abstract** Populus euphratica has important practical significance for the ecological stability and safety of the mainstream of Tarim River. In order to understand the distribution of populus euphratica, taking the high-resolution remote sensing images as the main data source, combining with the field survey and the statistical methods, we analyzed the area, land type and spatial distribution characteristics of populus euphratica in different sections of the Tarim River from 2010 to 2015, which could provide some information services for the restoration and protection of populus euphratica. The results show that ① the populus euphratica in the main stream of Tarim River shows a trend of shrinking, the change area are mainly concentrated in the upstream and midstream of main river, and the area of populus euphratica in the downstream of Tarim River is less changed. ② From the perspective of the spatial change type, the area of populus euphratica transforming into cultivated land is the largest, accounting for 97.56% of the change area. The phenomenon of transforming into cultivated land is more obvious in Yuli, Shaya and Luntai. ③ The variation area of populus euphratica are concentrated in the area within 2 km from the river channel, and with the increase of the distance from the river, the area of variation area decreases.

**Key words** populus euphratica, spatial variation characteristic, land type, overlay analysis, the mainstream of Tarim River (Page: 48)

### Realization of 3D Virtual Scene of Ancient Buildings in the Scenic Spot Based on MapGIS and SketchUp Platform

by WU Hongbo

**Abstract** In order to strengthen the inheritance and development of ancient buildings, taking Datang Furong Garden of Xi'an City for example, we used the 3D modeling technologies of MapGIS platform and SketchUp to realize the fine modeling of 3D structure of ancient buildings. And then, we constructed and released the 3D model and virtual scene of the ancient buildings in the MapGIS platform, and realized the spatio-temporal dynamic display of the virtual landscape and the 3D visualization of the ancient buildings in the scenic spot. The results show that the MapGIS platform not only realizes the fine modeling and batch modeling of structural units of the complex building, but also achieves the integration of 3D virtual scenes and real scenes and interactive analysis and query of 2D/3D data, which can provide visual technical support for development planning and smart management of tourist scenic spot. The 3D modeling technology is the basis of intelligence of the scenic spot. The integration of virtual scene and the real 3D historic building model will not only attract more tourists' attention, but also promote the service standard of the tourist scenic spot.

**Key words** geographical information, fine modeling, 3D scene, virtual technology, scenic spot, ancient building (Page: 52)

### Urban Flood Susceptibility Assessment in the Middle and Lower Reaches of the Yangtze River Based on GIS

by LIU Na

**Abstract** In this paper, we used the daily temperature and rainfall observation data of 73 national weather stations in the middle and lower reaches of the Yangtze River basin from 1980 to 2017 to analyze the change characteristics of daily temperature and rainfall in the flood season of past 40 years. Combining with the meteorological and urban characteristics, we established the evaluation index system of urban flood susceptibility, and realized the detailed and spatialized calculation of the evaluation indexes in the study area based on GIS. We used the fuzzy comprehensive evaluation method to establish the evaluation model, and corrected the weight by analytic hierarchy process to realize the evaluation of urban flood susceptibility in the middle and lower reaches of the Yangtze River basin. The results show that the total storm rainfall in the middle and lower reaches of the Yangtze River basin decreases first and then increases, and increases significantly after 2008. The average daily temperature and the number of high temperature days have been on the rise since 1980, and the rising trend is obvious. Urban flood very high susceptibility areas are mainly concentrated in the southern Anhui-northeastern Jiangxi-eastern Hubei, Shanghai, Nanjing, Hangzhou and central Hunan. The low susceptibility areas are mainly concentrated in the northwestern Hubei-southwestern Henan-southern Shaanxi, southwestern Hunan-southeastern Guizhou, and Wuxi, Suzhou, Chuzhou.

**Key words** the middle and lower reaches of the Yangtze River, urban flood, GIS, susceptibility (Page: 57)

### Water Information Extraction of Nanjing City Based on Sentinel-1A Data

by CHEN Yuanqian

**Abstract** Based on the advanced Sentinel-1A SAR data, we extracted the water information of Nanjing City. Firstly, we preprocessed the SAR images by filtering, radiation correction and geometric correction. And then, we used the gray level co-occurrence matrix to extract the texture information, and combining with the scattering intensity information, implemented the initial classification by SVM algorithm. Finally, we used terrain information to extract mountains, then removed the mountain shadow from the initial classification to obtain the final water extraction result. Through comparison experiments, it is found that the method can effectively remove the influence of the mountain shadow and the paddy field during the flooding period, and make the result closer to the real surface. This study can provide a corresponding theoretical support for the water resource management department of Nanjing City.

**Key words** SAR, water information extraction, texture feature, DEM, SVM (Page: 62)

### GPS Time Series Analysis in South Tibet

by XUE Tianyun

**Abstract** In this paper, we used the GAMIT/GLOBK software package to calculate 58 GPS continuous observation stations and 41 mobile observation stations in south Tibet from 2011 to 2017, and obtained the high precision coordinate sequence of these sites under ITRF2008. And then, we used the results of GRACE inversion to correct the seasonal term of the time series of GPS stations, and the

results showed that the weighted root mean square (WRMS) of three components (E, N, U) were reduced by 15.52%, 26.41% and 45.06% respectively. According to the characteristic value of PCA, we used the first principal component to calculate the common mode error, and the result showed that a large part of the periodic term in the GPS time series could be attributed to the common mode error. Finally, we used the variance component estimation method to quantitatively calculate the noise characteristics and obtained the accurate velocity field.

**Key words** time series, GRACE, common mode error, noise, velocity field (Page: 66)

### Research on Road Update Methods in Construction of One Map on Navigation

by HOU Ailing

**Abstract** One map on navigation of Hubei Province is an important part of one map on Beidou high precision navigation and location service and one map on Smart Hubei spatio-temporal information cloud platform. The fineness and current of road network data are of great significance to the construction of one map on navigation. In this paper, we selected five methods to update the vectors and properties of roads, in order to ensure the current of the road network data of one map on navigation.

**Key words** one map on navigation, road network data, orthoimage, information system, large scale data (Page: 70)

### Design and Implementation of Weather Service Guarantee System for Bicycle Racing Based on WebGIS

by SHI Hairui

**Abstract** Aiming at the business requirements of the meteorological service modernization in international road bicycle racing, using the service-oriented B/S four-tier architecture, based on WebGIS, information visualization and other technical means, we combined geospatial data, weather forecast and actual weather, and designed a weather service guarantee system for bicycle racing. And then, we introduced the function modules, system architecture design and main technologies of this system in detail. In the application process of meteorological service business in bicycle racing, the system shows good business application effect, and improves service quality.

**Key words** WebGIS, bicycle racing, weather service, GPS (Page: 73)

### Quick Update and Loading Elements into Database Based on Change Detection

by CHEN Chao

**Abstract** In this paper, we proposed a quick method of update and loading elements into the database based on change detection. Firstly, we acquired the homogeneous image segments of the current remote sensing images under the restriction of historic vector data, and constructed the feature space and rule sets according to different features to achieve feature extraction. And then, we obtained increment data by realizing an overlay analysis between extracted features and background vector data. Finally, we loaded the increment data into the historical database with different methods. Experimental result shows that the extraction accuracy of important river system and playground can reach 0.867 and 0.8 respectively. So this method can be an effective measure for the quick update of basis geographical information, provide the reference datum for the update of geographical conditions data.

**Key words** homogeneous image segment, feature space, change detection, overlay analysis, increment loading (Page: 77)

### Design of Earthquake Disaster Risk Estimation System Based on HAZUS

by LU Jiyun

**Abstract** Based on the technical requirements and system application requirements of earthquake disaster risk estimation, we analyzed the present situation of earthquake disaster loss estimation at first. And then, we put forward the overall design of earthquake disaster risk estimation system based on HAZUS earthquake model, which was a widely used earthquake disaster loss estimation system in the world. In order to meet the needs of earthquake disaster risk estimation at different levels, the system adopted modular function design and multi-user version design, and taking network map data as the analysis data, highlighted the link between disaster reduction countermeasures and practical work of earthquake prevention and disaster reduction.

**Key words** HAZUS, earthquake disaster, risk estimation, system design (Page: 80)

### Application of EGM2008 and Beidou Foundation Augmentation System in Engineering Measurement

by LI Yuzhong

**Abstract** In this paper, we examined the accuracy of the Beidou foundation augmentation system and the global EGM2008 gravity model in the actual projects, and attempted to adopt the new field operation mode of "Internet + Location (Beidou)". The result shows that the elevation accuracy of the EGM2008 model can reach 1.2 cm in the region after the correction of the datum plane gap. The difference between the Beidou foundation augmentation system and the JSCORS in the experimental area is less than 3 cm.

**Key words** Beidou foundation augmentation system, EGM2008 gravity model, elevation anomaly, JSCORS (Page: 84)

### Application of Surveying and Mapping New Technologies in Land Change Investigation

by WANG Nan

**Abstract** Land change investigation is to investigate the current situation of land use change, to update the land investigation database, and to maintain current status of land investigation data, which can provide the basic information for the daily management of land and resources "approval, supply, use, supplement and inspection", as well as economic and social development. How to acquire land change data quickly, efficiently and with high quality is the core content of this work. Using aerial surveying and on-demand mapping of UAV to obtain high quality working basic map, developing real-time survey data acquisition and transmission software based on Android, and developing land change investigation